Adhesion and separation models for direct hydrophilic bonding

E. Navarro, Y. Bréchet, A. Barthelemy, I. Radu, J.-P. Raskin, and T. Pardoen

Citation: Journal of Applied Physics **117**, 085305 (2015); doi: 10.1063/1.4913481
View online: http://dx.doi.org/10.1063/1.4913481
View Table of Contents: http://scitation.aip.org/content/aip/journal/jap/117/8?ver=pdfcov
Published by the AIP Publishing

Adhesion and separation models for direct hydrophilic bonding

E. Navarro,[1,2] Y. Bréchet,[2] A. Barthelemy,[1] I. Radu,[1] J.-P. Raskin,[3] and T. Pardoen[4]
[1]*SOITEC—Parc Technologique des Fontaines, 38190 Bernin, France*
[2]*SIMaP—Grenoble-INP, 1340 rue de la Piscine, 38402 St. Martin d'Hères, France*
[3]*Institute of Information and Communication Technologies, Electronics and Applied Mathematics (ICTEAM), Université catholique de Louvain, B-1348 Louvain-la-Neuve, Belgium*
[4]*Institute of Mechanics, Materials and Civil Engineering (iMMC), Université catholique de Louvain, B-1348 Louvain-la-Neuve, Belgium*

(Received 20 November 2014; accepted 5 February 2015; published online 24 February 2015)

A simple model describing the hydrophilic adhesion between solid surfaces, with low roughness is proposed to explain both the influence of the interface roughness and quantity of water present at the interface on the work of adhesion and work of separation. The observed hysteresis between adhesion and separation is explained by the evolving distribution of water along the bonding interface. This model is based on earlier molecular dynamics simulations of hydrophilic direct bonding previously obtained by Cole *et al.* An experimental validation is presented showing good agreement with model predictions. © *2015 AIP Publishing LLC*.
[http://dx.doi.org/10.1063/1.4913481]

I. INTRODUCTION

Adhesion constitutes a very wide multidisciplinary field of research with numerous practical impacts on our daily life from adhesion tapes, water capillarity, or natural biological systems such as Gecko lizard toe pads.[1]

Direct adhesion between solids is commonly used as a fabrication technique for transferring a thin film from a wafer to another, for instance, for the fabrication of Silicon-On-Insulator wafers (SOI).[2] Therefore, understanding the fundamentals of adhesion and developing predictive models for the fracture toughness of the interface is an important and challenging task.

For hydrophilic bonding, adhesion between solids occurs through a few mono-layers of water molecules which are adsorbed on the surface covered by hydroxyl groups (–OH).[3] Then, a network of strong oxygen mediated hydrogen bonds is formed between the two solids.

In order to produce effective direct adhesion, the roughness of the surfaces has to be very low, i.e., about 1 – 2 Å RMS in case of silicon oxide surface formed on standard silicon wafers.[2]

The effect of surface topology on adhesion is usually studied while considering the elastic deformation of the surface asperities.[4–8] However, for very low surface roughness, considering the elastic deformation of the surface may not be appropriate because the thickness of the water layer present at the interface is on the same order of magnitude as the surface topological variations. The diameter of one water molecule diameter is about 3 Å.

Miki *et al.* use the bearing ratio, which describes the fractional area lying above a given depth, in order to derive the effective contact area as a function of the roughness without considering any elastic deformation.[9]

The silicon oxide/water/silicon oxide system has been previously studied using molecular dynamics simulations.[10–13] Nevertheless, the usual simulation box is not large enough in the surface in-plane directions, typically about 30 × 30 Å, to account for the surface roughness.

Moreover, the effect of relative humidity, i.e., the quantity of water present at the interface, has been observed to impact the interface adhesion dynamics.[14] An hysteresis effect has been reported between the adhesion and the separation processes a few minutes after the interface creation, even at room temperature.[15] This effect cannot be explained by the well-known interface aging observed only many hours after the interface creation.[16]

Therefore, a model for hydrophilic adhesion is needed, at a micrometer scale and for surfaces having very low roughness. In this paper, we propose a simple model accounting for the surface roughness and for the amount of adsorbed water in order to predict the work of adhesion and of separation.

The model deals with adhesion occurring through hydrogen bonds only, corresponding to the very beginning of the hydrophilic direct bonding process, when no covalent bonds are present at the interface.

The difference between the work of adhesion and separation is explained by the movements of the water molecules along the bonding interface. The work of adhesion is defined as the energy per unit area gained by the formation of the interface, and the work of separation or bonding energy corresponds to the opening of the interface.

This model is primarily motivated by earlier molecular dynamics results obtained by Cole *et al.* concerning the hydrophilic bonding of silicon and silicon oxide surfaces.[12] The adhesive or repulsive forces have been evaluated as a function of the interface gap and as a function of the quantity of water.

In order to determine what are the different length scales playing a role in the adhesion of two surfaces, a portion of an experimental AFM profile, the thickness of one monolayer of water and the box size of the molecular dynamics simulation are compared in Fig. 1. In addition, the AFM tip is schematically represented, to scale, by an ellipse.

Some assumptions can be made when looking at Fig. 1. First, the surface topology is extremely flat, meaning that the curvature of the surface should not have an effect on the

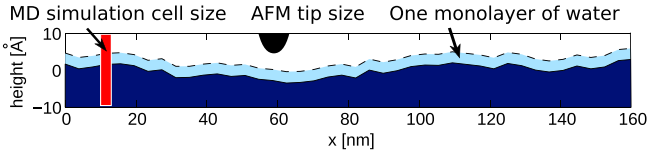

FIG. 1. The dark area is a small part of an experimental AFM profile. The measurement points are located $\Delta x \approx 40$ Å apart (2 μm long scan for 512 points). The dashed line represents one monolayer of water molecules (3 Å) and the rectangle represents the box size of the molecular dynamic simulation ($30 \times 30 \times 20$ Å^3). The AFM tip radius is typically about 10 nm. The x-axis scale is ten times larger than the z-axis scale. The roughness value for the entire AFM scan (2×2 μm^2) is about 1 Å RMS.

behavior of the water layer, and its thickness and chemical state, should be uniform over the wafer surface. However, once the interface is closed, the interface gap height is expected to play an important role, since a constraint is added on the local thickness of the water layer. Second, the silica (or silicon) material can be considered non-deformable, as long as one or a few monolayers of water are present between the two surfaces. Third, the molecular dynamics simulation cell is too small to properly describe the surface roughness obtained from AFM measurement.

The main idea of the model is to average the forces obtained by molecular dynamics simulations over the interface gap height variation.

II. THEORETICAL CONSIDERATIONS

A. Description of the model

In the following, the local separation distance between the two surfaces is called z. The amount of water filling the gap is quantified by the number of mono-layers, noted ML. The force between the two surfaces, at a nanometer scale, is noted $f_{nm}(z,ML)$. The magnitude of these forces is extracted from Fig. 8 in Ref. 12.

The roughness of a surface is usually defined as the root mean square value (RMS) of the surface height statistical distribution. In case of bonding, the interface gap height has to be considered, which is given by the statistical distribution of the spacing between the two surfaces in front of one another. Then, the interface roughness σ is defined as the standard deviation (i.e., the root mean square value) of the interface gap height distribution, and it is determined from the two surface roughnesses σ_1 and σ_2 by the relationship: $\sigma^2 = \sigma_1^2 + \sigma_2^2$, with both surfaces topographies assumed to be uncorrelated.

The height distribution of the surface, hence of the bonding interface, is well described by a Gaussian distribution,

$$G(z,\,\sigma) = \frac{1}{\sigma\sqrt{2\pi}}\exp\left(-\frac{z^2}{2\sigma^2}\right). \tag{1}$$

Two cases are distinguished in the interface model: the first corresponds to the adhesion of the two surfaces and the second corresponds to the separation of the interface. The difference between both cases is related to the water distribution along the bonding interface. Fig. 2 is a schematic representation of the bonding interface before contact (a), just after contact (b), and before separation (c).

Before bonding, water is assumed to be uniformly distributed over the wafer surface (Fig. 2(a)). As discussed before, the variation of the surface topography is too small to have an effect on the water coverage distribution. When the two surfaces are brought into contact, the water layer is, in some regions, undergoing compression and at other regions undergoing tension (Fig. 2(b)). Because the water layer consists of only a few mono-layers of molecules, the movement of the water along the interface is assumed slower than the characteristic time of the bonding, i.e., the water does not flow along the interface during the bonding process, hence some regions of the water molecular layers can undergo tension. The molecular dynamics simulations provide the attractive or repulsive forces as a function of the gap height and as a function of the quantity of water molecules. Then, by imposing mechanical equilibrium, the average distance between the two surfaces just after contact and, from this, the work of adhesion can be calculated.

A few instants after the creation of the interface, the water is expected to move (diffuse) along the bonding interface in order to reduce the energy of the entire system. Then, the water coverage everywhere along the surface will be a function of the gap height between the two surfaces (Fig. 2(c)). The work of separation can be calculated, in this case, using as input values the results of the molecular dynamics simulation.

The details of the model derivation are presented in the following, both for the adhesion and separation cases.

B. Adhesion model

The idea is to compute the average force between the two substrates as a function of the average gap separation distance z for a given amount of water ML_0 and for a given interface roughness standard deviation σ. Because the model considers a surface size in the micrometer range, the average force is noted $F_{\mu m}$,

$$F_{\mu m}\,(z,\,\sigma,\,ML_0) = \int_{-\infty}^{+\infty} G(z'-z) f_{nm}\,(z',\,ML_0)\,dz'. \tag{2}$$

Mechanical equilibrium corresponds to an average force equal to zero for a gap opening z_{eq} such that

$$F_{\mu m}(z_{eq},\,\sigma,\,ML_0) = 0. \tag{3}$$

Finally, the work of adhesion W is obtained as the work performed by the microscopic forces when the two surfaces are brought in contact from an infinite separation distance to the equilibrium distance z_{eq},

$$W(\sigma,\,ML_0) = -\int_{z_{eq}}^{+\infty} F_{\mu m}\,(z,\,\sigma,\,ML_0)\,dz. \tag{4}$$

The work of adhesion can be, therefore, estimated as a function of the interface roughness σ and as a function of the amount of water at the interface ML_0. Integration and root finding are performed numerically, using MATLAB®, from the

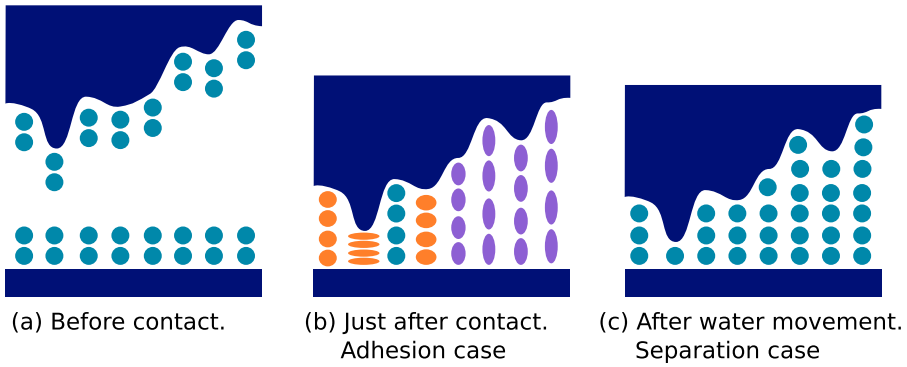

FIG. 2. Schematic representation of the bonding interface. Plain circles represent monolayer of water molecules; (a) before surfaces are brought in contact, they are covered by an uniform layer of water; (b) configuration just after the bonding of the two surfaces. The water layer undergoes compression at some surface points (flat ellipses) and is under stretching at other points (elongated ellipses). The work of adhesion is calculated using this configuration as reference; (c) after some time, the water distribution along the interface becomes non uniform. The local amount of water is then a function of the local interface gap in such a way that the global system energy is minimized. The work of separation is calculated using this configuration as reference.

interpolated values proposed by Cole *et al*. The results are shown in Fig. 3.

C. Separation model

After the interface is closed, the water is expected to diffuse along the bonding interface in order to reduce the system energy. Therefore, the quantity of water ML_{eq} at a certain location along the surface will be a function of the interface gap height at this point, noted z, in such a way that $f_{nm}(z,ML_{eq}) = 0$.

For simplicity, the equilibrium quantity of water ML_{eq} is considered to be a linear function of the gap height: $ML_{eq} = z/t_{water}$, where t_{water} is the thickness of one monolayer of water (≈3 Å). This assumption will be discussed later.

Because the bonding interface is considered as a closed system, the entire amount of water remains a constant. Its value is noted ML_0. If the amount of water is not enough to fill the entire interface gap, the equilibrium quantity of water ML_{eq} could not be satisfied for all possible surface locations. Hence, two configurations have to be distinguished, depending whether there is enough water to entirely fill the interface gap or not (see Fig. 4).

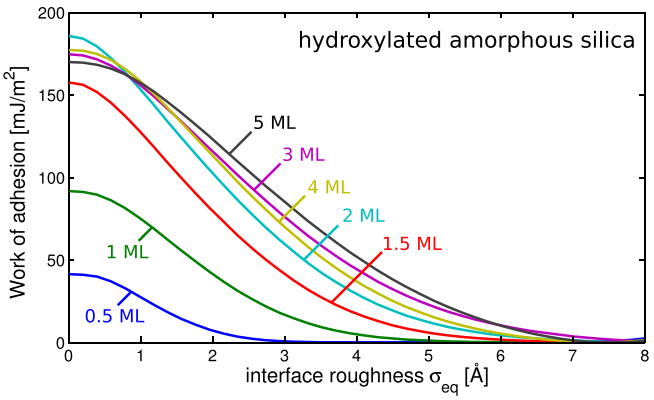

FIG. 3. Theoretical work of adhesion calculated from the molecular dynamics results and by considering the interface roughness σ and the amount of water at the interface ML_0 (these values are twice those given by Cole *et al*. because, in the present work, both surfaces are considered).

In case of a large amount of water (Fig. 4(a)), the average gap separation between the two surfaces z_{eq} is determined by: $z_{eq}^{(a)} = ML_0\, t_{water}$. Indeed, because the statistical height distribution is symmetric around the average height value, the amount of water above the mean value is the same as the quantity missing below the mean value.

In this case, the macroscopic work of separation, noted $E_{\mu m}^{(a)}(\sigma, ML_0)$, is obtained by averaging the nanoscopic work of separation $E_{nm}(ML_{eq})$ over the interface gap height distribution,

$$E_{\mu m}^{(a)}(\sigma, ML_0) = \int_{-\infty}^{+\infty} E_{nm}\left(\frac{z - z_{eq}^{(a)}}{t_{water}}\right) G(z,\sigma)\, dz, \qquad (5)$$

where the nanoscopic work of separation $E_{nm}(ML)$ is obtained from the molecular dynamics results (see Fig. 9 in Ref. 12).

The case of a small quantity of water is more complex because "hard" contacts are expected to occur between the two surfaces (see Fig. 4(b)). The "hard" contact corresponds to the configuration where no intermediate water layer is present between the two surfaces, i.e., there is a direct adhesion through hydroxyl groups or covalent bonds. In this case, the average separation distance between the two surfaces $z_{eq}^{(b)}$ is determined by the interface area undergoing "hard" contact. This issue is related to the rough surface adhesion models, taking into account the elastic deformation of the

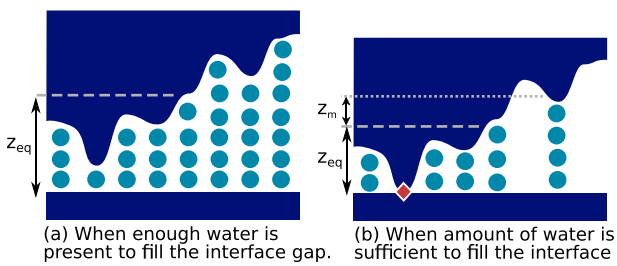

FIG. 4. Schematic representation of the bonding interface after rearrangement of the water to minimize energy. (a) Configuration where the water layer entirely fills the interface gap. (b) Configuration when not enough water is present to fill the entire interface gap. In consequence, "hard" contact occurs at some points of the interface (diamond symbol).

surfaces. For simplicity, the average separation distance is fixed arbitrarily to $z_{eq}^{(b)} = 3\sigma$, meaning that about 0.13% of the surface is undergoing a "hard" contact.

Because there is not enough water to fill the entire interface gap, some voids are expected to be present in the areas where the interface gap is the largest. It is assumed that the water fills first the small interface gaps, until a certain maximum gap height, noted z_m.

Therefore, the maximum height z_m is calculated by solving the equation,

$$z_m \quad \text{such that} \quad ML_0 = \int_{-z_{eq}^{(b)}}^{z_m} \frac{z - z_{eq}^{(b)}}{t_{water}} G(z,s)\, dz. \tag{6}$$

The macroscopic work of separation, noted $E_{\mu m}^{(b)}$, is obtained by averaging the nanoscopic work of separation $E_{nm}(ML)$ over the interface gap height distribution, but, now, the integration range is limited by the constraint of constant amount of water, i.e., from $-z^{(b)}$ to z_m,

$$E_{\mu m}^{(b)}(\sigma, ML_0) = \int_{-z_{eq}^{(b)}}^{z_m} E_{nm}\left(\frac{z - z_{eq}^{(b)}}{t_{water}}\right) G(z,\sigma)\, dz. \tag{7}$$

Finally, the choice of case (a) instead of case (b) is determined by the following condition:

$$ML_0 > \int_{-z_{eq}^{(b)}}^{+\infty} \frac{z - z_{eq}^{(b)}}{t_{water}} G(z,\sigma)\, dz. \tag{8}$$

Similar to the adhesion problem, integration and root finding are performed numerically. The results are shown in Fig. 5.

III. EXPERIMENTAL VALIDATION

The bonding propagation velocity and bonding interface energy (i.e., the work of separation) have been measured for different silicon oxide surface roughness.

A 1 μm-thick silicon oxide layer was thermally grown on 200 mm-diameter silicon wafers. The oxide layer was then etched by using a diluted hydrofluoric acid solution (HF) in order to roughen the surfaces before bonding. Three types of surfaces have been elaborated: Type A with no oxide was removal, Type B after etching over a depth of 150 nm and Type C after etching over a depth of 600 nm. The surface roughness was measured using a NanoScope DIM3000 AFM from Veeco Metrology in tapping mode on $2 \times 2\,\mu m^2$ scan. The AFM noise is estimated equal to 0.5 Å. Values equal to $\sigma_A \approx 1.0$ Å, $\sigma_B \approx 2.4$ Å, and $\sigma_C \approx 3.5$ Å are measured. Therefore, permutations of the surface type allow testing up to six different interface roughnesses (AA, AB, BB, AC, BC, and CC).

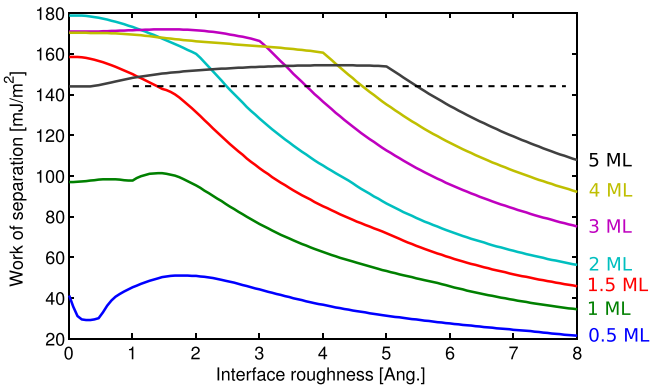

FIG. 5. Variation of the theoretical work of separation calculated from the molecular dynamics results as a function of the interface roughness for different amounts of water at the interface (these values are twice those given by Cole *et al.* because, in the present work, both surfaces are considered). The dashed line indicates twice the surface tension of water (144 mJ/m^2).

The work of adhesion W can be roughly estimated from the bonding velocity v using the relationship: $W = \beta v^{5/4}$, where β is a constant.[17] The value of the constant is estimated equal to $\beta \approx 6.5 \times 10^{-3}$ J m$^{-3/4}$s$^{-5/4}$ according to a previous study[18] ($v = 2.4$ cm/s and $W = 112$ mJ/m^2). It is worth mentioning that the bonding velocity depends on the bonding configuration and on the location along the wafer. For this experiment, the bonding propagation velocity was recorded using an infrared light observation system. The bonding initiation was performed at the wafer edge, and the bonding velocity was taken at the center of the wafer.

The bonding energy is measured using the usual blade insertion method.[19,20] The open crack length is measured using infrared light transmission images and the beam formula is used despite the circular wafer geometry. For this reason, a large error is expected on the estimation of the bonding interface energy.

It is worth mentioning that the wafer bonding step as well as the interface energy measurements are performed in a clean room environment where the relative humidity is about 40%.

The measured variations of the work of adhesion and of the bonding interface energy as a function of the interface roughness are shown in Fig. 6.

The work of adhesion is found to decrease with the interface roughness from about 140 mJ/m^2 down to 40 mJ/m^2. The interface energy for separation decreases from about 160 mJ/m^2 down to 100 mJ/m^2.

The work of adhesion appears to be more sensitive to the roughness than the interface energy (separation). According to the model, the rearrangement of water along the interface allows compensating for the roughness effect by filling the interface gap.

In addition, the model predictions for 1 *ML* and 2.5 *ML* (i.e., 2 and 5 monolayers of water at the interface) are plotted on both adhesion and separation plots (Figs. 6(a) and 6(b), respectively). A relatively good agreement is obtained between the general theoretical predictions and the measurements, especially when considering the simplification of the model and the experimental uncertainty.

IV. DISCUSSION

In the following, a more detailed discussion about the model hypotheses and future model improvements is presented.

One of the main assumptions of the model is that the characteristic time of the water flow movement along the interface is larger than the characteristic time of the interface

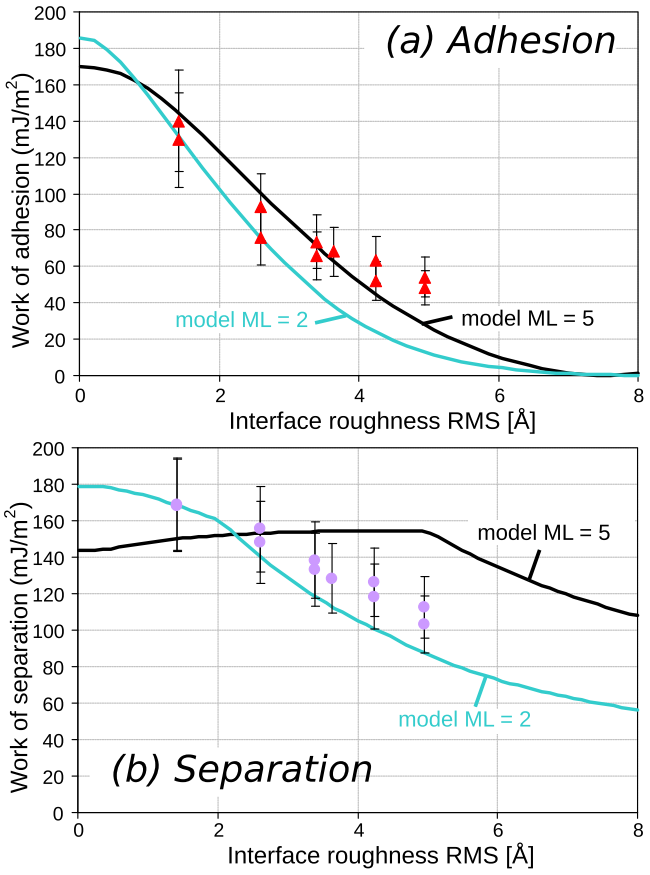

FIG. 6. Theoretical and experimental results about the interface roughness effect on (a) the work of adhesion and (b) the work of separation. The solid line is the model predictions for the quantity of water $ML = 2$ and $ML = 5$ at the interface.

bonding. Considering a bonding velocity $v = 2\,\mathrm{cm/s}$ and a self-diffusion coefficient of water $D_{H_2O} \approx 2 \times 10^{-9}\,\mathrm{m^2\,s^{-1}}$ at 25 °C,[21] the characteristic length scale at which both characteristic times are equal is $L = D_{H_2O}/v \sim 0.1\,\mu\mathrm{m}$. The lateral length scale of the surface is assumed to be greater than $0.1\,\mu\mathrm{m}$. Therefore, water diffusion along the interface is expected not to contribute to the work of adhesion, i.e., to the bonding front propagation, while it contributes to the bonding interface toughness as long as the opening occurs some time after the interface bonding contact (between some milliseconds to some seconds).

In the separation model, the quantity of water at equilibrium ML_{eq} is assumed to linearly depend on the gap separation distance. According to the molecular dynamics simulation results, this assumption is valid for more than 1 *ML* per surface. Below this value, the equilibrium separation gap remains almost constant. However, defining the gap separation distance for a small water coverage is not straightforward since the water molecules, the hydroxyl groups, and the last layer of silicon oxide can be all mixed together at about the same height value. In addition, effects related to the discrete nature of the water may be possible, i.e., a more complex function, for example, a step function, may be preferable.

Considering only the total amount of water may be not sufficient to describe the entire chemical state of the interface. The hydroxyl group density, as the chemical state of the surface, could constitute additional input parameters for the model.

Another hypothesis used for the separation model is that the large interface gaps are free of water molecules. It is not obvious that, even for large gaps, a small quantity of water will not remain adsorbed on hydroxyl groups. In this case, the derivation of the entire quantity of water should be modified. The extreme case of this situation looks like the capillary adhesion between rough surfaces where bridges of water form between the two surfaces leading to existence of liquid/void interfaces.[22]

V. CONCLUSION AND PERSPECTIVES

A model for hydrophilic bonded interface is proposed, taking into account the interface micro-roughness and the distribution of water along the bonding interface. The model is based on previous molecular dynamics simulations obtained by Cole *et al*. The hysteresis effect between the adhesion and the separation of the interface is explained by the different distribution of water along the bonding interface. The experimental results are coherent with the model predictions.

The model can be used as a starting point to build a quantitative description of interface aging, including covalent bonds formation and water diffusion through silicon oxide. However, since both water molecules and covalent bonds will be present at the interface, and that the interface energy measurement involves stress on the interface, the stress corrosion effect will have to be considered.

[1]H. Gao, X. Wang, H. Yao, S. Gorb, and E. Arzt, "Mechanics of hierarchical adhesion structures of geckos," Mech. Mater. **37**(23), 275–285 (2005).
[2]Q.-Y. Tong and U. Gösele, *Semiconductor Wafer Bonding: Science and Technology* (John Wiley, New York, 1999).
[3]R. Stengl, T. Tan, and U. Gösele, "A model for the silicon wafer bonding process," Jpn. J. Appl. Phys. **28**(part 1), 1735–1741 (1989).
[4]J. A. Greenwood and J. B. P. Williamson, "Contact of nominally flat surfaces," in *Proceedings of the Royal Society of London. Series A. Mathematical and Physical Sciences* (1966), Vol. 295, Issue 1442, pp. 300–319.
[5]K. N. G. Fuller and D. Tabor, "The effect of surface roughness on the adhesion of elastic solids," in *Proceedings of the Royal Society of London. A. Mathematical and Physical Sciences* (1975), Vol. 345, Issue 1642, pp. 327–342.
[6]D. Maugis, "On the contact and adhesion of rough surfaces," J. Adhes. Sci. Technol. **10**(2), 161–175 (1996).
[7]C. Gui, M. Elwenspoek, N. Tas, and J. G. E. Gardeniers, "The effect of surface roughness on direct wafer bonding," J. Appl. Phys. **85**(10), 7448–7454 (1999).
[8]F. Rieutord, H. Moriceau, R. Beneyton, L. Capello, C. Morales, and A.-M. Charvet, "Rough surface adhesion mechanisms for wafer bonding," ECS Trans. **3**(6), 205–215 (2006).
[9]N. Miki and S. M. Spearing, "Effect of nanoscale surface roughness on the bonding energy of direct-bonded silicon wafers," J. Appl. Phys. **94**(10), 6800–6806 (2003).
[10]D. Timpel, M. Schaible, and K. Scheerschmidt, "Molecular dynamics studies of silica wafer bonding," J. Appl. Phys. **85**(5), 2627–2635 (1999).
[11]D. A. Litton and S. H. Garofalini, "Modeling of hydrophilic wafer bonding by molecular dynamics simulations," J. Appl. Phys. **89**(11), 6013–6023 (2001).
[12]D. J. Cole, M. C. Payne, G. Csányi, S. Mark Spearing, and L. Colombi Ciacchi, "Development of a classical force field for the oxidized Si surface: Application to hydrophilic wafer bonding," J. Chem. Phys. **127**, 204704 (2007).

[13]S. Leroch and M. Wendland, "Simulation of forces between humid amorphous silica surfaces: A comparison of empirical atomistic force fields," J. Phys. Chem. C **116**(50), 26247–26261 (2012).
[14]D. B. Asay and S. H. Kim, "Effects of adsorbed water layer structure on adhesion force of silicon oxide nanoasperity contact in humid ambient," J. Chem. Phys. **124**(17), 174712 (2006).
[15]D. S. Grierson and K. T. Turner, "Characterization of hysteresis of surface energy in room-temperature direct bonding processes," ECS Trans. **33**, 573–580 (2010).
[16]G. A. C. M. Spierings, J. Haisma, and T. M. Michelsen, "Surface-related phenomena in the direct bonding of silicon and fused-silica wafer pairs," Philips J. Res. **49**(1), 47–63 (1995).
[17]F. Rieutord, B. Bataillou, and H. Moriceau, "Dynamics of a bonding front," Phys. Rev. Lett. **94**(23), 236101 (2005).
[18]E. Navarro, Y. Bréchet, R. Moreau, T. Pardoen, J.-P. Raskin, A. Barthelemy, and I. Radu, "Direct silicon bonding dynamics: A coupled fluid/structure analysis," Appl. Phys. Lett. **103**(3), 034104 (2013).
[19]W. P. Maszara, G. Goetz, A. Caviglia, and J. B. McKitterick, "Bonding of silicon wafers for silicon-on-insulator," J. Appl. Phys. **64**(10), 4943–4950 (1988).
[20]Y. Bertholet, F. Iker, J. P. Raskin, and T. Pardoen, "Steady-state measurement of wafer bonding cracking resistance," Sens. Actuators A **110**, 157–163 (2004).
[21]M. Holz, S. R. Heil, and A. Sacco, "Temperature-dependent self-diffusion coefficients of water and six selected molecular liquids for calibration in accurate 1h nmr pfg measurements," Phys. Chem. Chem. Phys. **2**(20), 4740–4742 (2000).
[22]M. P. de Boer and P. C. T. de Boer, "Thermodynamics of capillary adhesion between rough surfaces," J. Colloid Interface Sci. **311**(1), 171–185 (2007).